Lander and rover histories of dust accumulation on and removal from solar arrays on Mars

Ralph D Lorenz, German M Martínez, Aymeric Spiga, Alvaro Vicente-Retortillo, Claire E Newman, Naomi Murdoch, Francois Forget, Ehouarn Millour, Thomas Pierron

Planetary and Space Science 207 (2021) 105337

Contents lists available at ScienceDirect

Planetary and Space Science

journal homepage: www.elsevier.com/locate/pss

Lander and rover histories of dust accumulation on and removal from solar arrays on Mars

Ralph D. Lorenz [a,*], German M. Martínez [b,c], Aymeric Spiga [e], Alvaro Vicente-Retortillo [d,h], Claire E. Newman [g], Naomi Murdoch [f], Francois Forget [e], Ehouarn Millour [e], Thomas Pierron [e]

[a] Space Exploration Sector, Johns Hopkins Applied Physics Laboratory, Laurel, MD, 20723, USA
[b] Lunar and Planetary Institute, Universities Space Research Association, Houston, TX, USA
[c] Dept of Climate and Space Sciences and Engineering, University of Michigan, Ann Arbor, MI, USA
[d] Centro de Astrobiología (INTA-CSIC), Madrid, Spain
[e] Laboratoire de Météorologie Dynamique/IPSL, Sorbonne Université, CNRS, Ecole Normale Supérieure, PSL Research University, Ecole Polytechnique, 75005, Paris, France
[f] Institut Supérieur de l'Aéronautique et de l'Espace (ISAE-SUPAERO), Université de Toulouse, Toulouse, France
[g] Aeolis Research, Chandler, AZ, USA
[h] Dept of Climate and Space Sciences and Engineering, University of Michigan, Ann Arbor, MI, USA

ARTICLE INFO

Keywords:
Solar power
Dust
Dust devils
Mars
Boundary layer meteorology

ABSTRACT

The degradation in electrical output of solar arrays on Mars landers and rovers is reviewed. A loss of 0.2% per Sol is typical, although observed rates of decrease in 'dust factor' vary between 0.05% and 2% per Sol. 0.2%/Sol has been observed throughout the first 800 Sols of the ongoing InSight mission, as well as the shorter Mars Pathfinder and Phoenix missions. This rate was also evident for much of the Spirit and Opportunity missions, but the degradation there was episodically reversed by cleaning events due to dust devils and gusts. The enduring success of those rover missions may have given an impression of the long-term viability of solar power on the Martian surface that is not globally-applicable: the occurrence of cleaning events with an operationally-useful frequency seems contingent upon local meteorological circumstances. The conditions for significant cleaning events have apparently not been realized at the InSight landing site, where, notably, dust devils have not been detected in imaging. Optical obscuration by dust deposition and removal has also been observed by ultraviolet sensors on Curiosity, with a similar (but slightly higher) degradation rate. The observations are compared with global circulation model (GCM) results: these predict a geographically somewhat uniform dust deposition rate, while there is some indication that the locations where cleaning events were more frequent may be associated with weaker background winds and a deeper planetary boundary layer. The conventional Dust Devil Activity metric in GCMs does not effectively predict the different dust histories.

1. Introduction

The occurrence of global dust storms visible even from Earth attests to the vigor of the Martian atmospheric dust cycle, e.g. (Kahre et al., 2017). In addition to being a key factor in the Martian climate, influencing atmospheric and surface temperatures and thus the surface/atmosphere exchange of water and carbon dioxide, dust is of vital importance in spacecraft operations. This can be true even of radioisotope-powered vehicles, since science operations may require adequate visibility, and thermal control can be affected by dust deposition. But dust is most obviously and profoundly important for solar-powered landers and rovers, both due to dust suspended in the atmosphere, and that drizzles onto spacecraft surfaces like solar arrays. The specific problem of power loss due to dust accumulation on Mars solar arrays has been the subject of experimental consideration for at least three decades (e.g. Gaier et al., 1991).

Dust attenuation of solar array output was first observed on the Mars Pathfinder mission (and its Sojourner rover), but the mission was short in duration and so the power loss was not a major mission constraint. Similarly, dust deposition on some surfaces had been noticed in imaging observations of the radioisotope-powered Viking landers over their long surface operation, but was inconsequential. The Pathfinder experience,

* Corresponding author.
E-mail address: Ralph.lorenz@jhuapl.edu (R.D. Lorenz).

https://doi.org/10.1016/j.pss.2021.105337
Received 22 May 2021; Received in revised form 6 August 2021; Accepted 31 August 2021
Available online 2 September 2021

where about 0.25% per Sol loss in power was seen, set expectations for the Mars Exploration Rovers (MER) Spirit and Opportunity. The projected decline in power defined the nominal mission lifetime to be 90 Sols (i.e. it was a capability-driven requirement – e.g. Lorenz, 2019). In fact, this expectation proved to be pessimistic, as we discuss later, and these missions operated for thousands of Sols. The environmental challenge to the InSight mission, however, where the arrays have become steadily more and more dust-covered (Fig. 1) and array output has fallen after one Mars year to about a quarter of that at landing (e.g. Lorenz et al., 2021) shows that the MER experience of dust removal (Fig. 2) is not universally-applicable, but may be contingent upon the local meteorological conditions and/or the specifics of the solar panel (e.g. surface properties, motion-induced vibration). The possible lack of cleaning events at Elysium was hinted at in a pre-landing survey of dust devil tracks (Reiss and Lorenz, 2016), see also (Perrin et al., 2020). The present paper critically reviews the solar array performance on landed Mars missions to document the record of dust deposition and removal.

2. Observations

Solar array currents are an essential and routine element of spacecraft housekeeping data, but historically have not been routinely made openly available, appearing only in graphical form in sporadic papers often in the engineering literature (see later). However, because of the sensitivity of its geophysical measurements (seismometers and magnetometers), the InSight mission included solar array data in its public data archive. In addition to the current data gathered from the literature on Mars Pathfinder, the Mars Exploration Rovers Spirit and Opportunity, the Phoenix lander and InSight, we include photocurrent data from the ultraviolet sensors on the REMS instrument on Curiosity. Although this is an instrument rather than a power-generating system, the function here (to measure light transmission through a glass cover on which atmospheric dust settles) is the same. The datasets are presented in Fig. 3 and are available at http://lib.jhuapl.edu.

The traditional format of reporting dust accumulation is a "Dust Factor", indicating the ratio of the measured power output to that of an array without any dust. It should be understood that strictly this ratio is specific to a given solar array and illumination condition, in that different solar cell technologies respond to different wavelengths of light. Furthermore, the intensity and spectral distribution of the direct and diffuse (scattered) components of light incident on the solar panel vary with the solar elevation and the amount of dust in the atmosphere (expressed as an optical depth or 'tau' (τ) – which is itself strictly a wavelength-dependent quantity). However, for practical purposes, the best measurement of array output is at the diurnal maximum, typically around noon if the array is perfectly horizontal, and in conditions where tau is low enough that the direct illumination dominates. Thus most estimates of 'dust factor' can be reasonably compared between missions, although dust storm conditions with tau in excess of unity, or near-polar missions like Phoenix where the sun is always low in the sky, may have systematic differences in what dust factor results from a given deposition of a given dust. We now discuss the various datasets in turn.

The photocurrent measurements on InSight are reported with a resolution better than 0.1% near noon at the start of the mission, allowing practical detection of transient variations of $<0.3\%$ (e.g. Lorenz et al., 2020). As the solar array output has declined, however, the effect of the quantization noise in the current measurement has proportionately increased. No formal uncertainty estimate is calculated for the Dust Factors presented here, but it may be noted that the retrieval of the dust factor relies on an estimate of tau, which is typically determined from camera images (e.g. Lemmon et al., 2015) with a precision of ~ 0.1 compared to a typical value of 0.7. The optical depth tau can also include a significant contribution from water ice clouds, which can be highly variable. The absolute value of the dust factor is probably then only determined to an accuracy of a few per cent, although the point-to-point precision in dust factor when tau is known to be nearly constant may approach 1%. In any case, the digitization of some of the datasets presented here from published figures is likely only good to about 2%, and

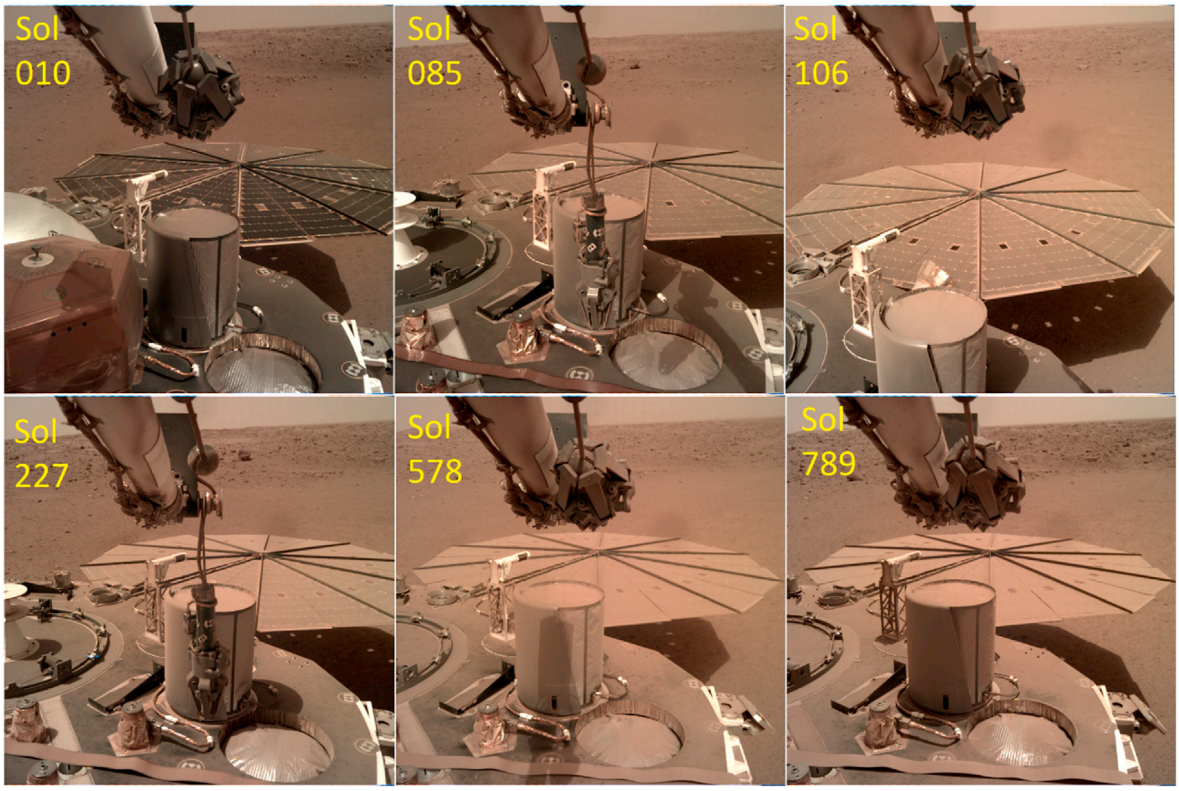

Fig. 1. Steady accumulation of dust on the InSight solar arrays (Lorenz et al., 2021).

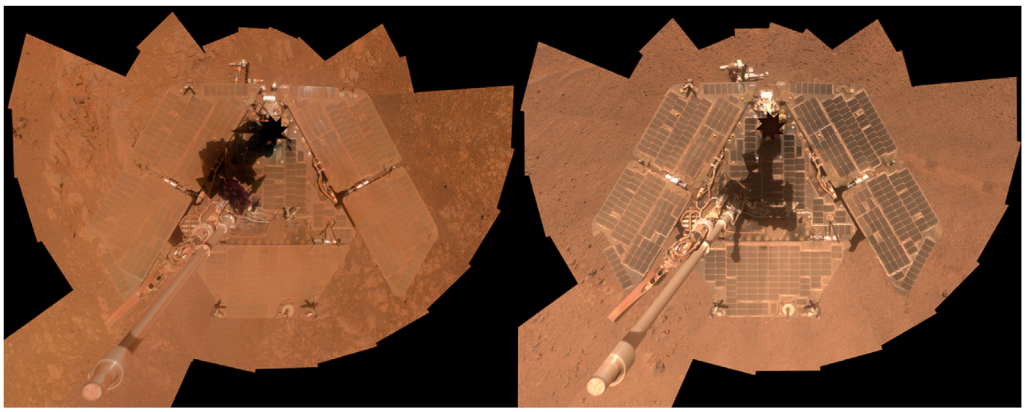

Fig. 2. A self-portrait of NASA's Mars Exploration Rover Opportunity taken in late March 2014 (right) shows that much of the dust on the rover's solar arrays has been removed since a similar portrait from January 2014 (left). Both were taken by Opportunity's panoramic camera (Pancam). Image Credit: NASA/JPL-Caltech/Cornell Univ./Arizona State Univ.

we suggest this estimated precision be adopted in any consideration of the significance of results.

We report the dust factor evolution as a decay rate d. Thus the evolution of solar array current I(t) (corrected for tau) is of the form $I(t) = I(0)\exp(-dt)$, where t is the time in Sols. Appendix 1 provides further detail on the metrics and noise considerations.

2.1. Mars Pathfinder

Observations of the progressive reduction of the Sojourner rover's solar array output due to dust deposition on Mars were initially reported by the Pathfinder Team (1997) and further examined by Landis and Jenkins (2000). This Materials Adherence Experiment recorded the short-circuit current of a single cell with a transparent cover which could be temporarily retracted, by a small shape-memory actuator, to give a covered/uncovered difference measurement indicating accumulation of dust on the cover. This investigation showed an approximately 0.28% per Sol decline until the experiment actuator ceased function.

A later report (Crisp et al., 2004) documented the output of the Pathfinder lander's solar arrays (a single cell being set up as a short-circuit current monitor). In principle, the dust factors could be different in the two experiments for the same dust coating, since the Sojourner and Pathfinder cells were different. Furthermore, since the cells on the rover and on the lander were exposed to slightly different environments, their dust coating evolutions might have differed slightly. However, the reported histories appear broadly speaking to be the same. Crisp et al. (2004) suggests that the evolution could be described by two linear segments, with the decline becoming smaller after Sol 20, although we could interpret the data as a more or less constant ~0.25% per Sol decline, with some number of cleaning events in the sol 39–52 period. It is of interest that the largest vortex pressure drops reported (Murphy and Nelli, 2002) were on Sols 34 and 39, although the incomplete observation record makes strong conclusions difficult. The observed overall decline in output was consistent with some estimates of dust fallout that had been made before the mission (Landis, 1996), and set expectations for the Mars Exploration Rover missions.

2.2. Mars Exploration Rovers – Spirit and Opportunity

The power systems of the Mars Exploration Rovers (MERs), which landed in 2004, are described in Stella et al. (2005). Their surface performance through Sol 2100 is documented in Stella and Herman (2010). As is now well-known, while the initial decline of solar array output was consistent with expectations, the downward trend of array dust factor abruptly reversed in 'cleaning events', and camera images showed the arrays to have become less dusty.

These cleaning events were suspected of being strong gusts, and possibly dust devils. The dust devil attribution for the majority of Spirit events was confirmed by Lorenz and Reiss (2015) who showed first that the timing of the Spirit cleaning events coincided with the onset of 'dust devil season' as indicated by the rover cameras (L_s = 173–355°), and second that the recurrence interval of cleaning events was consistent with the encounter rate of convective vortices detected as pressure drops by landed meteorology stations, extrapolated to the pressure drop (and thus wind intensity) commensurate with dust lifting thresholds measured in the laboratory.

The dust factor evolution is thus somewhat like a 'sawtooth', with a steady decline punctuated by quasi-regular instantaneous jumps. The seasonal signal is rather prominent in the Spirit record (Fig. 4), with large jumps in dust factor occurring during dust devil season in three successive Mars years (once L_s~170°, and in two other years at L_s~255°). The Opportunity record appears to have a somewhat more complex seasonal pattern, but with a weaker amplitude. The Curiosity record is rather regular, with cleaning observed L_s~220–300° in all three years (Vincente-Retortillo et al., 2018).

It is of interest to consider how lander and rover dust histories would have evolved in the absence of clearing events. This can be explored given the time series by numerically removing the events, as follows, to generate an 'uncleaned' history.

We take the Opportunity dust factor time series DF(i) and construct a 'corrected' history CDF(i) as if no cleaning occurred, as follows.

CDF(0) = DF(0) = 1.0
For i = 1 to N
IF DF(i)≥DF(i-1) THEN CDF(i) = CDF(i-1)
IF DF(i) < DF(i-1) THEN CDF(i) = CDF(i-1)*DF(i)/DF(i-1)
NEXT

This procedure yields the 'rectified' or 'uncleaned' histories shown in Fig. 5, and in semi-logarithmic form in Fig. 6. Although the linear Fig. 5 facilitates comparison with the raw histories in Fig. 3, it de-emphasizes the data later in the respective missions, since the dust factor values all become small. The semi-logarithmic portrayal of Fig. 6, on which exponential decay appears as a straight line, shows that a 0.2% per Sol decay describes the data very well, except for Curiosity after Sol 600 or so, where a 0.4% per Sol decay applies.

It is seen (Fig. 5) that for both Spirit and Opportunity we obtain the rather uniform exponential decay of 0.2% per Sol, except for a couple of bumps which were only temporary reprieves.

Some rather severe episodes of accumulation are noted – e.g. a decline of 0.9 to 0.55 from Sol 1230 to 1270, about 1.2% per Sol.

NB The methodology here may slightly overestimate the long-term

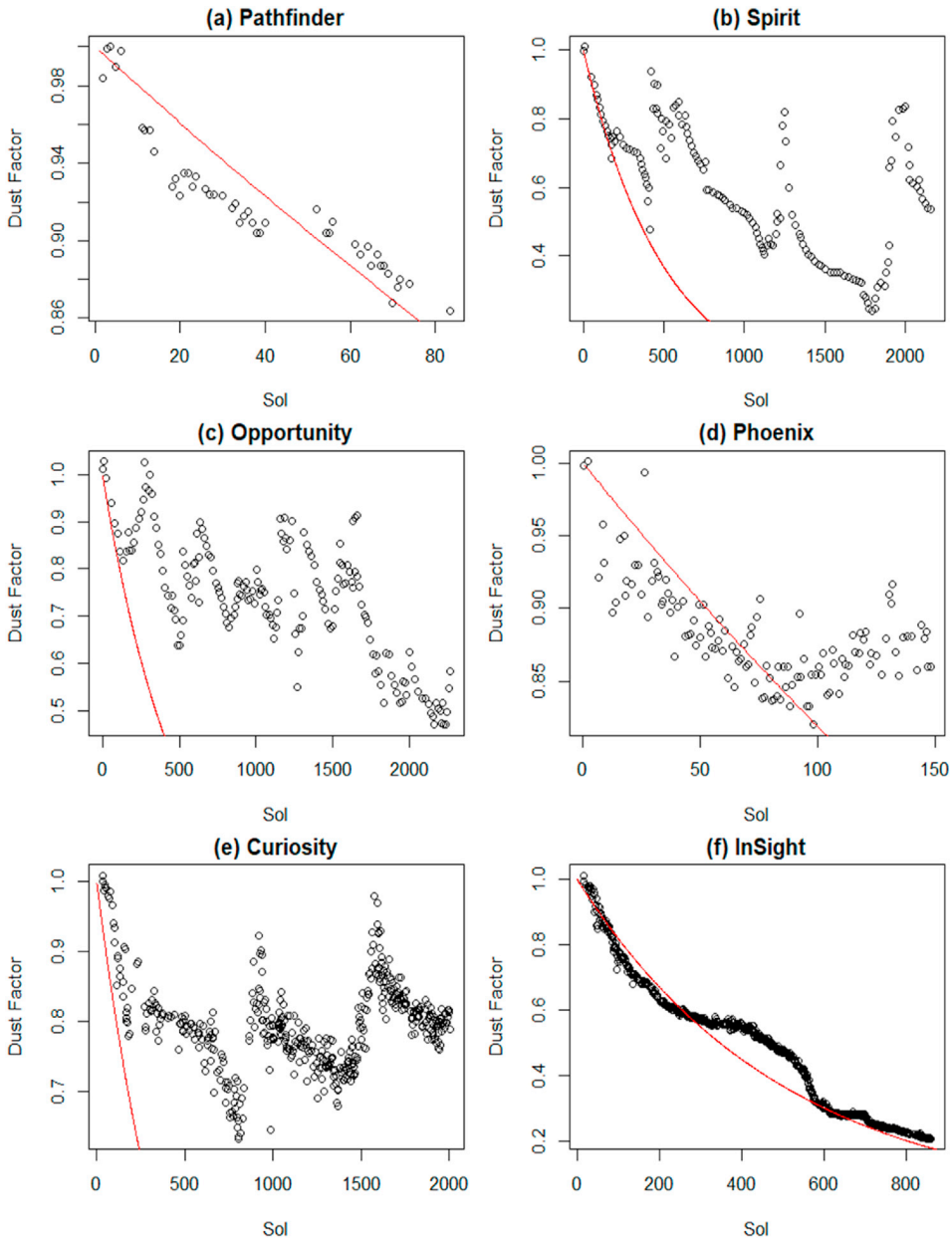

Fig. 3. Dust transmission factors from landed Mars missions in chronological order of landing a-f. Note the different time and transmission scales. The thin red line shows a 0.2% per Sol exponential decline.

accumulation in that the determination of the dust factor is noisy, and the logic in the no-removal history 'rectifies' this noise leading to an inevitable accumulation. However, the effect cannot be large overall, since segments of the uncorrected record can be fit quite well with the same exponential decay (e.g. decay to ~0.47 in first 410 Sols implies ~0.18%/Sol).

2.3. Phoenix

Drube et al. (2010) document the decline in dust factor on the 151-Sol Phoenix lander mission. The array dust factor history is also shown, together with some details of the spacecraft power system, by Coyne et al. (2009).

The Phoenix mission appears to be something of an outlier, perhaps not coincidentally given its high latitude (68°N). The trend for the first 100 Sols (Fig. 3d) was of the order of 0.15% per Sol, but then the dust factor leveled out and in fact steadily climbed. The period after Sol 95 was associated with higher levels of vortex and dust devil activity (revealed by pressure drops and camera images respectively, Ellehoj et al., 2010), suggesting that these may have led to dust removal from the solar panels. Since the record was relatively short, and the dust factor variations quite small and affected somewhat by measurement and digitization noise (variations of 1% or less are not well-determined) we have not constructed an 'uncleaned' history.

2.4. Curiosity

Although the Curiosity rover itself is powered by a Multi-Mission Radioisotope Thermoelectric Generator (MMRTG) and not solar arrays, photodiode sensors have been used to detect dust devil shadows and to monitor the accumulation and removal of dust from the sensor windows, e.g. Vicente-Retortillo et al. (2018). That paper used a smoothed record of dust factors. The raw record, containing more information on cleaning events is shown here (Fig. 3e), and has been processed to yield an

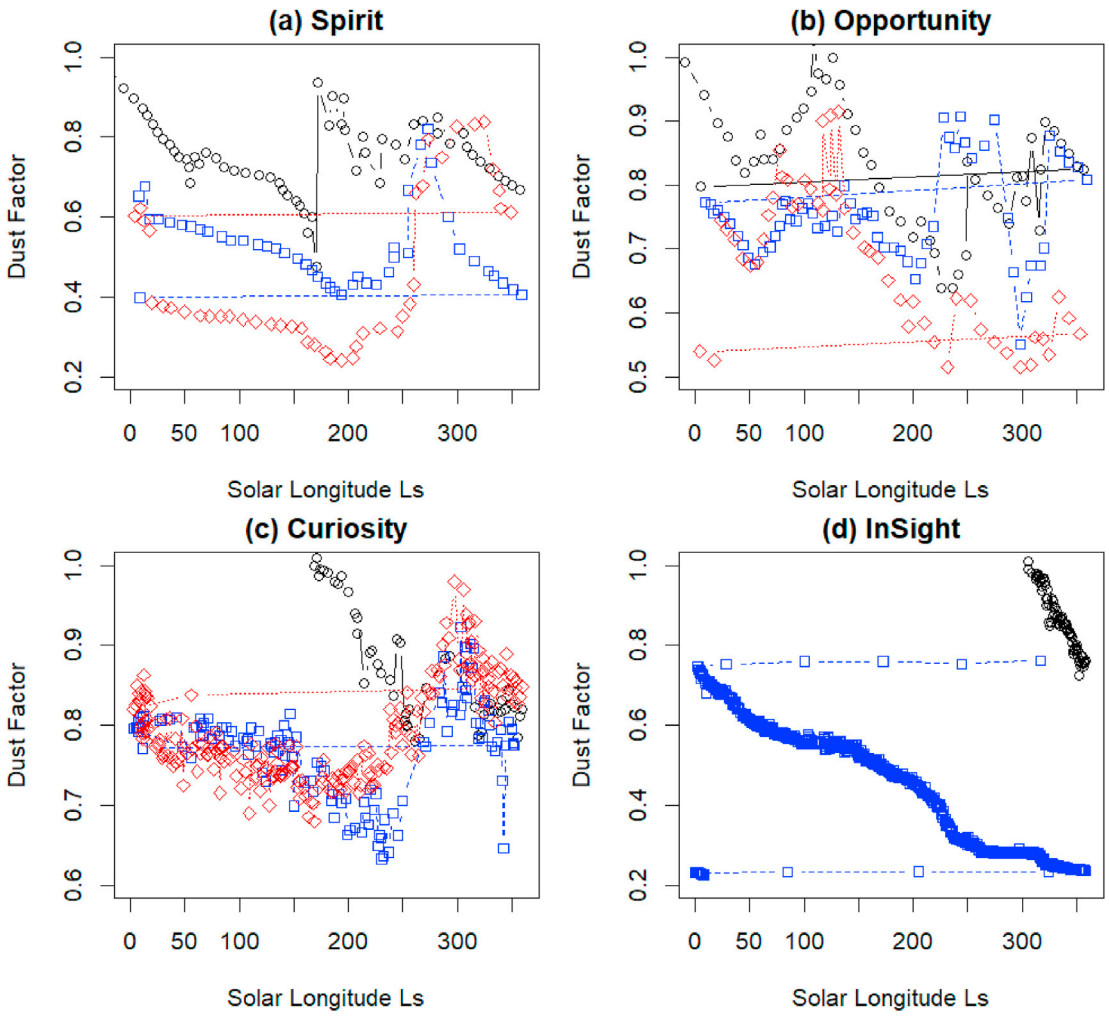

Fig. 4. Long-lived lander array dust factors plotted as a function of Mars season (L_s – solar longitude equal to 0 at Vernal Equinox, 90 at northern summer solstice, etc.). The Spirit pattern is strongly seasonal with large dust removal in southern summer. Opportunity has a somewhat repeating but more complex pattern, with removal in summer and winter, and accumulation at both equinoxes. The Curiosity pattern is annually rather repeatable. The black, blue and red symbols denote dust factors in the first, second and third Mars year, respectively.

'uncleaned' history in Fig. 5c.

Vicente-Retortillo et al. (2018) noted that a broadly seasonal accumulation and removal cycle occurred, rather similarly to the Spirit rover. Although UV flux might be expected to be more sensitive to dust absorption than the broader and redder spectrum that develops current in solar arrays, in fact the uncleaned dust factor evolution is initially the same as for the Mars Exploration Rovers, with a 0.2% per Sol initial accumulation.

Although not obvious in Fig. 5c, the semilogarithmic portrayal in Fig. 6c reveals that in the 2nd Mars year of the mission, the uncleaned accumulation rate appears to have been higher than in the first 600 or so Sols.

2.5. *InSight*

The evolution of the InSight solar array currents has been described by Lorenz et al. (2020, 2021). For details on the solar array design, and expectations on power evolution, see (Lam et al., 2016; Lisano and Kallemeyn, 2017). The Lorenz et al. (2021) report noted that the dust factor has undergone an essentially unmitigated decline of 0.2% per Sol, throughout the 800-Sol mission to date. In this respect, the raw dust factor history (Fig. 3f) and the 'uncleaned' one (Fig. 4d) are essentially the same. The declining power, which began to restrict scientific observations by around Sol 700, motivated an effort to remove dust by shaking the solar panels (see Appendix 2).

A notable feature of the InSight history is that the decline in array dust factor slows appreciably between Sols 200 and 400 before accelerating back to the overall expected trend. We discuss the meteorological circumstances behind this lull in section 5. The effects of a dust storm are noted in (Viúdez-Moreiras et al., 2020). Observations and circumstances of sediment movement recorded at the InSight landing site more generally are noted in (Baker et al., 2021; Charalambous et al., 2021).

3. Frequency and magnitude of cleaning events

Cleaning events can be detected in the dust factor time series by simple differencing, to identify positive steps in value. Although this procedure will report spurious detections at the few per cent level due to measurement noise, we prefer to avoid introducing ad-hoc filtering of the results, since the cumulative effect of even small cleanings can be significant in retarding the overall decline in dust factor. The time histories of cleaning events are shown in Fig. 7.

We can plot the frequency of cleaning events against their magnitude (see Fig. 8). This distribution, like other dust devil parameters, is highly skewed, favoring representation on logarithmic or semi-logarithmic axes. The straight-line character of the cumulative histograms on semi-logarithmic axes indicates that the events for all four datasets have an exponential distribution.

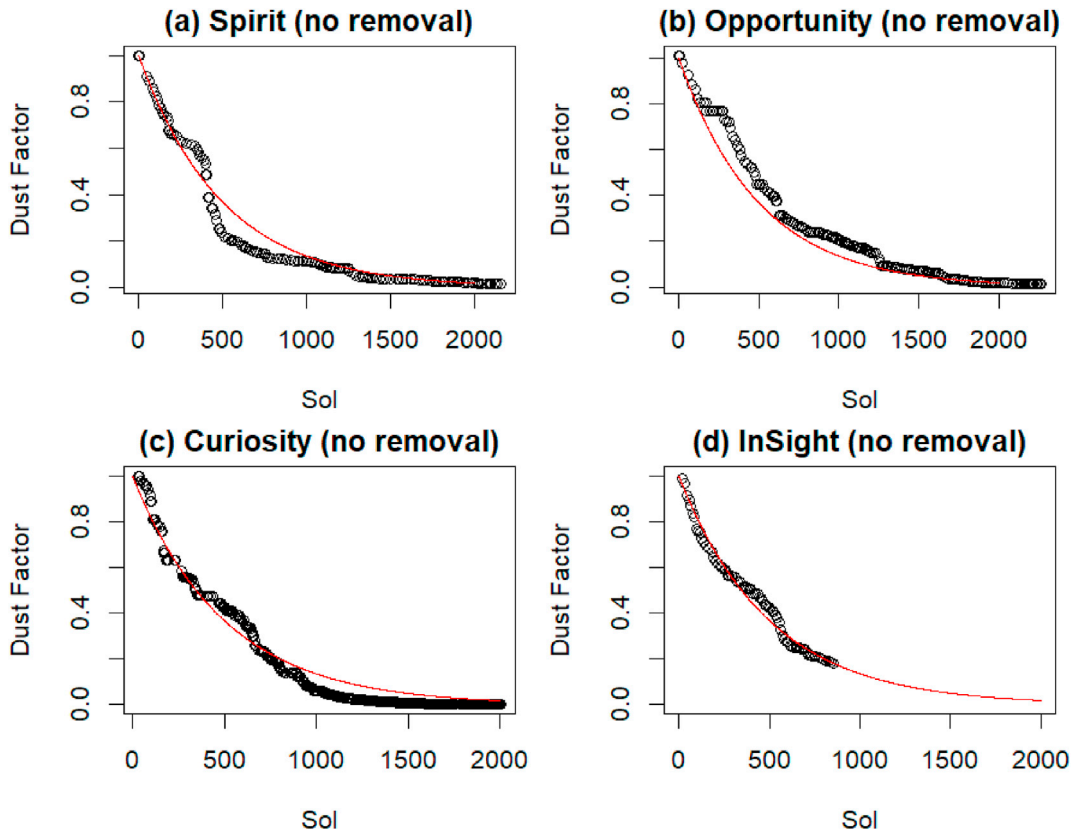

Fig. 5. 'Uncleaned' dust factor histories for the four long-duration missions from Fig. 3, shown on the same time and dust factor axes. All are broadly consistent with a steady 0.2%/Sol decline (thin red line), but it is evident that there are some periods when the accumulation is lower or higher than this.

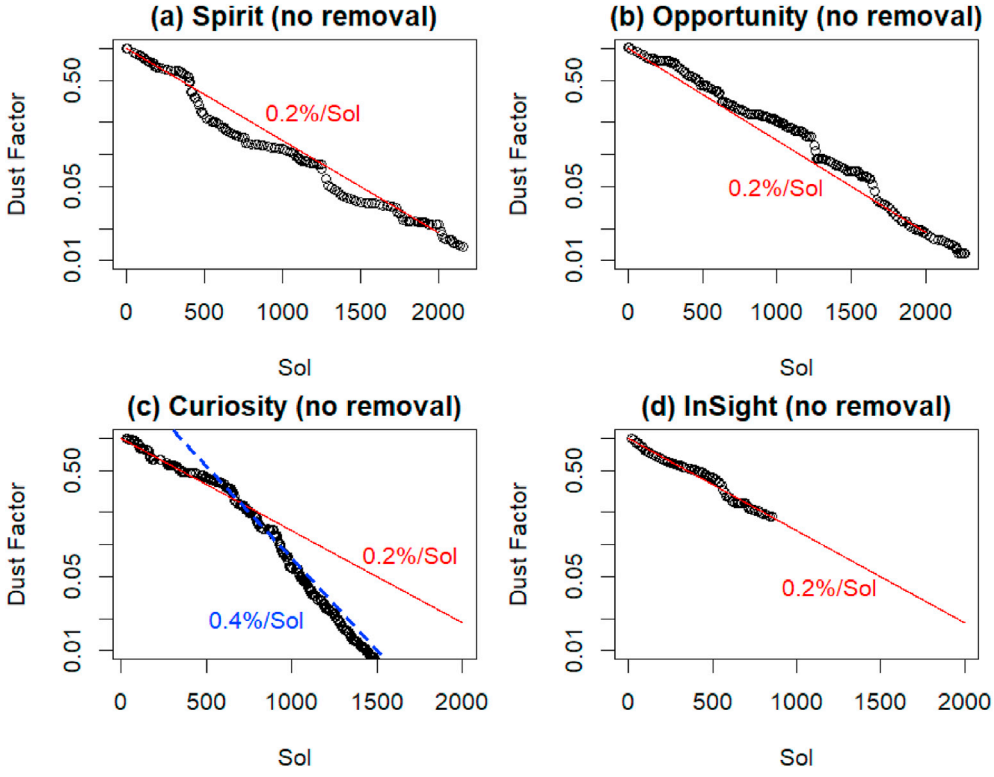

Fig. 6. Same 'uncleaned' histories as Fig. 5, but shown on a logarithmic y-axis to demonstrate the exponential decay at a near-universal 0.2% per Sol. The logarithmic portrayal avoids de-emphasizing the later data, and here highlights a change in behavior for Curiosity at about Sol 600, where the decay rate roughly doubles.

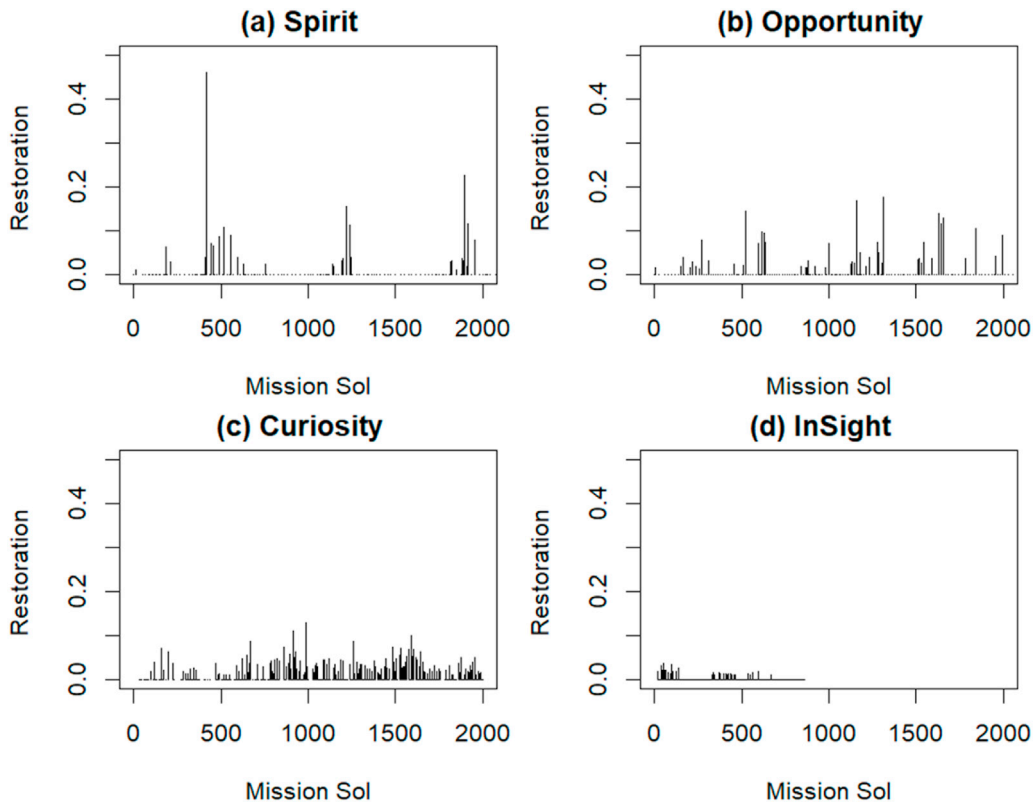

Fig. 7. Cleaning histories of the four long missions: plotted are the increments in dust factor versus time. The annual character of the Spirit events is prominent, as is the dearth of large events for InSight (for which many of the small spikes may be noise).

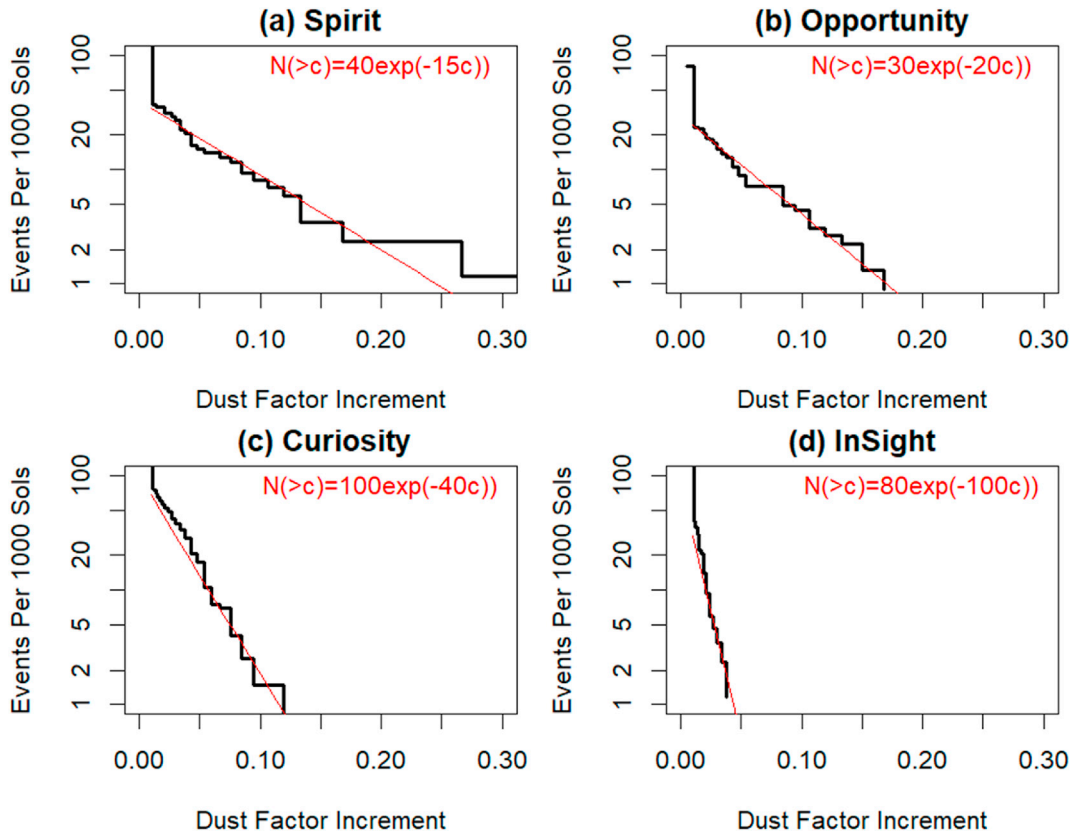

Fig. 8. Cumulative cleaning event recurrence rates as a function of increment in dust factor. The straight lines indicate an exponential distribution, with the expressions indicating number of events N per thousand sols with cleaning causing a dust factor increment greater than c.

It should be noted that while Figs. 5 and 6 show non-zero numbers of cleaning events for InSight, the vast majority are only one or two per cent, and may therefore indicate measurement noise. The retrieval of array dust factor relies on an optical depth estimate which is at best measured only daily, and in some cases must be interpolated between measurements some days apart. Thus when the actual optical depth changes on shorter timescales (and 1% level variations are reported even on only 10-min timescales, Lorenz et al., 2020) the dust factor may correspondingly be in error. Hence it is entirely possible that there were virtually no true cleaning events at all in the InSight data set. However, one ~1% cleaning event, albeit of only the outermost cells on the arrays, was documented on Sol 65 where a small step increase in array current occurred during a vortex encounter with a substantial pressure drop (Lorenz et al., 2020), so the number of cleaning events is not quite zero.

4. Variability of dust deposition rate

The dust factor histories can be interrogated by differencing to yield a set of dust factor variation rates. To avoid noisy results from differencing near-similar numbers, only decreases of dust factor of more than 0.01 are considered, and for the Curiosity and InSight data only every second and fifth datapoints are used. It is seen (Fig. 9) that the net accumulation rates (which may of course be accumulation mitigated by small removal events) for all the solar arrays peak between 0.15% per Sol and 0.3% per Sol.

The median values for Spirit, Opportunity, and InSight are (0.16, 0.18, 0.28) %/Sol, whereas the mean values (somewhat skewed by a handful of >1%/Sol values) are (0.39, 0.28, 0.34). Since the median values are more representative of what one will encounter in a given period, the mean of these (0.206%/Sol) is the best description of the decay for solar panels, although the variations mean there is little justification for a third or even second significant digit, hence this paper for succinctness describes the evolution as "0.2%/Sol".

The Curiosity rates appear to be higher (mean and median 0.36 and 0.51%/Sol respectively, only though 0.23 and 0.14%/Sol for the first 600 Sols). It may be that the actual dust deposition rates are higher at Gale than elsewhere, but it is also quite possible that because of the higher opacity of a given layer of dust in the ultraviolet compared to the solar array spectrum the dust deposition is the same or less.

5. Discussion

5.1. Differences in meteorological setting

The central question posed by this paper, noting the generally similar dust accumulation rates on four landed missions, but the quite different character of dust removal, is why this should be so? Or to put the question another way in the context of future missions to Mars, can the dust removal rate be predicted in advance based on location?

First, in terms of dust deposition, we use the Mars Climate Database (MCD) version 5.3 (see http://www-mars.lmd.jussieu.fr/) which is built by extracting monthly climatologies from reference simulations with the Laboratoire de Météorologie Dynamique [LMD] Global Climate Model (Forget et al., 1999). The GCM simulations make use of an interactive scheme for dust particles (Madeleiene et al., 2011) which accounts for atmospheric transport by resolved large-scale circulations, turbulent mixing, sedimentation and cloud microphysics (for which dust particles serve as condensation nuclei, and in turn the growth of the cloud particles help to scavenge the dust out of the atmosphere). The model follows the observed column dust optical depth, and predict the vertical distribution of the dust. On this basis, a diagnostic of the dust deposition rate on a flat horizontal plane at the surface of Mars ($kgm^{-2}s^{-1}$) is generated in the MCD. It should be recognized that like other MCD quantities, it corresponds to an average over a model grid cell (a 5.625° longitude by 3.75° latitude). It can be seen (Fig. 10) that there is relatively little variation between the predicted dust deposition rates for the different landers, which after all are mostly at similar latitudes. The notable exception is the Phoenix lander which has a lower dust deposition overall at its high

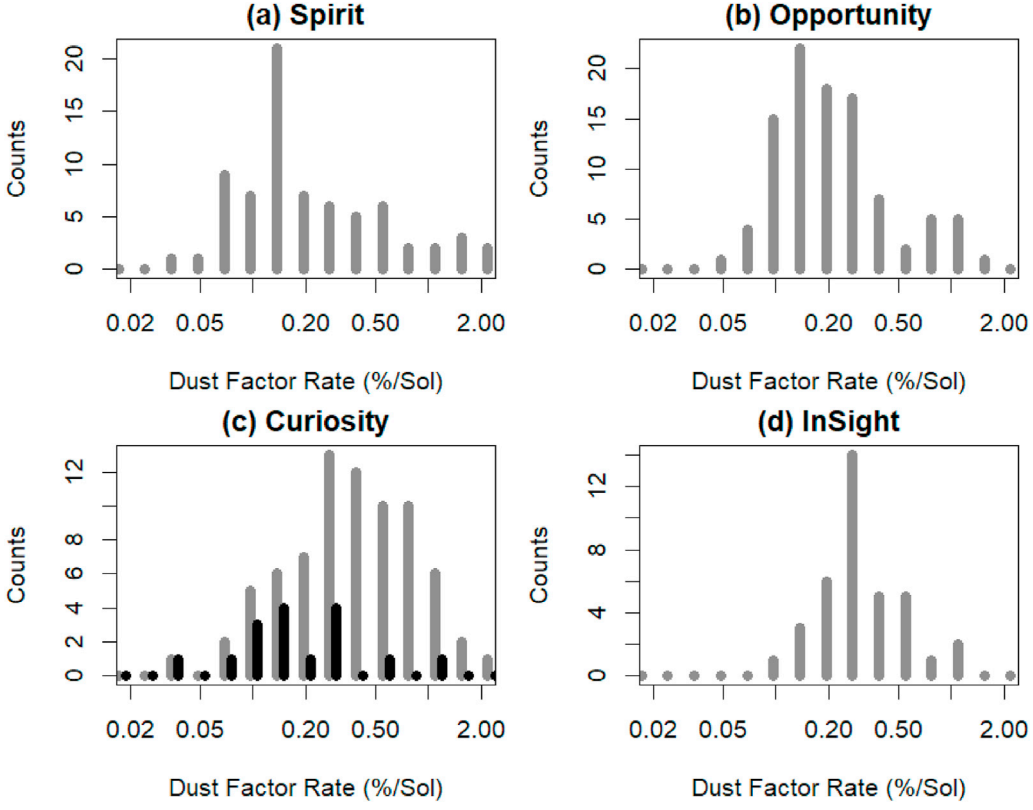

Fig. 9. The distribution of dust settling rates in $\sqrt{2}$-spaced logarithmic bins. In the third panel, the black bars show those settling rates measured in the first 600 Sols.

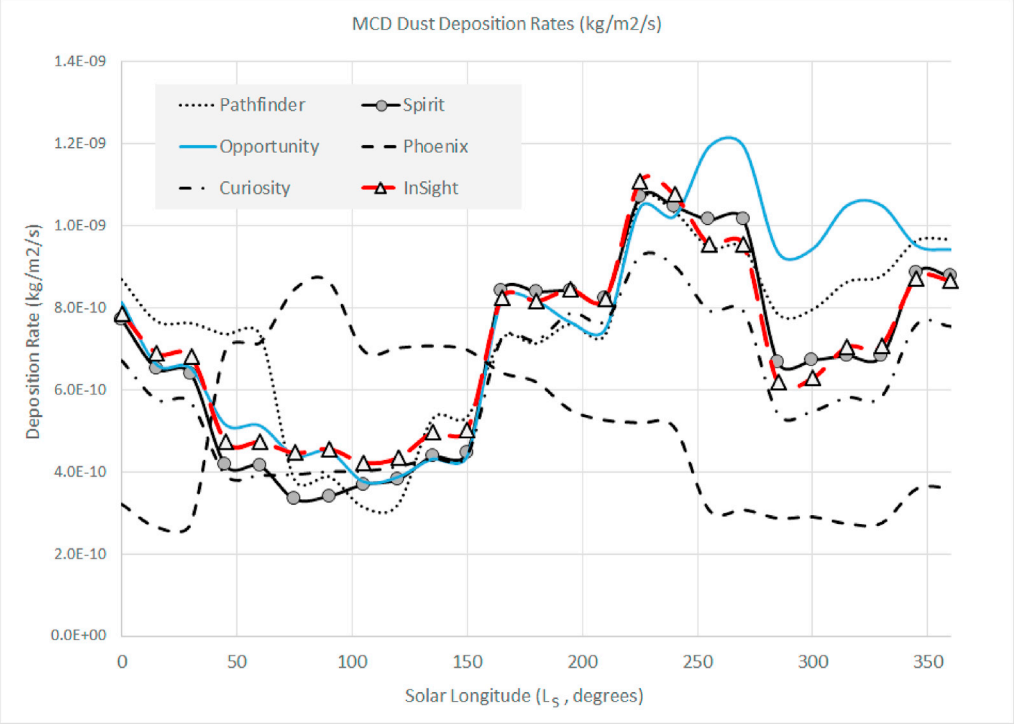

Fig. 10. Annual variation of regional dust deposition predicted by the MCD as a function of solar longitude (L_s). The cycles are fairly similar except for the high-latitude Phoenix lander.

latitude, while the seasonal variation is opposite to that of the others, with a minimum in the southern summer (L_s = 225–315°); this is of course of limited relevance for the present paper, in that the sun barely gets above the horizon at the Phoenix site in this season, hence solar power is in any case very low. The annual average dust deposition rates for the landers discussed in this paper are provided in Table 1. The fact that the predicted deposition rates for Spirit, Opportunity, Curiosity and InSight are very similar is consistent with the observed rates in Fig. 9.

It is a reasonable physical expectation that the higher the dust loading in the atmosphere, the higher the dust deposition rate (e.g. in Landis' (1996) original predictive model, or in the work of Yingst et al. (2020)). However, an examination of the atmospheric optical depth at the times at which the deposition rates were computed suggests (plots not shown) that the correlation is generally rather weak (R-squared < 0.15 for Spirit, Curiosity and InSight). Thus we do not find optical depth itself to be a strong predictor of dust accumulation on solar arrays. Again, this is unexpected because the gravitational deposition should be related to the amount of dust in the lower atmosphere, itself related to the column dust opacity. If no correlation is observed, this could mean that a process intensify the deposition of dust particles when the atmosphere is clearer. This cannot be related to the mean particle size of the dust particles since available observations show that the effective radius of dust particles is larger for higher dust opacity. One possibility could be related to the condensation of water ice at night in the atmosphere which is favored during periods of low dust loading (coating dust particles and accelerating sedimentation) or on the panel (enhancing the adhesion of dust).

Since even where abundant wind gust measurements exist at the local scale (e.g. at InSight, Baker et al., 2021) the exact circumstances of sediment mobilization are still under debate, a full exploration of the various meteorological parameters influencing the seasonal variation of dust removal at the various landing sites is beyond the scope of the present paper (see Martínez et al., 2017; Newman et al., 2021). However, convective vortices are suspected of being a principal factor. Some key meteorological quantities are indicated in Table 1 (we use these model results as a uniform basis for comparison, since in-situ wind measurements are not available for Spirit and Opportunity, and no uniform data for any lander exist for PBL depth and heat flux).

We compile in Table 1 the mean and maximum hourly winds from the MCD (noting that it may not fully capture the strong topographic effects at Gale crater), and from the MarsWRF model which is run at 2° (~120 km) horizontal resolution globally (which is sufficient to resolve the circulation at most landing sites) or in nested mesoscale mode giving 1.4 km resolution across Gale crater (used to resolve the topography of MSL's location). The MCD windspeeds are reported for a higher altitude than the MarsWRF model, and thus are systematically higher. The inter-site variation is similar, with Opportunity having the weakest winds and InSight the strongest (of the 4 long-duration sites).

We also report the "dust devil activity" (DDA) index based on the large scale atmospheric state predicted by the MarsWRF model. This quantity is based on a thermodynamic theory of Renno et al. (1998): despite the name, this theory applies equally to clear and dust-filled vortices. Full details of the theory and how it is applied to MarsWRF output may be found in e.g. Sect. 3.2 of Newman et al. (2019). In brief, convective vortices are modeled as convective heat engines, resulting in the DDA being set proportional to the sensible heat flux, F_s, multiplied by the vertical thermodynamic efficiency of the heat engine, η. The former depends primarily on the drag velocity and surface-to-air temperature difference, while the latter increases with the PBL depth.

Neither the average MCD surface eddy heat flux, nor the MarsWRF Dust Devil Activity index appear to explain the lack of dust removal at InSight compared with the other localities, although the PBL depth is lower there than at the other sites. PBL depth is an indicator of the height of dust devils on Mars (Fenton and Lorenz, 2016) although whether it is also an indicator of intensity (core pressure drop, and circumferential winds) has not been directly established. It is notable, however, that the background regional winds are considerably larger at InSight than the other long-lived landers: it has been speculated (Lorenz et al., 2021) that this background wind causes shear which prevents the formation of the largest and most intense dust devils, thereby suppressing cleaning events. However, note that wind speeds inside Gale crater may be stronger than

Table 1
Lander Location parameters. Note that MCD Winds (m/s) are the annual average and annual maximum of Monthly averages. The MCD Planetary Boundary Layer (PBL) depth is in km, and the dust deposition rate is in kg/m^2/s. The surface eddy heat flux is the kinematic flux in m/s/K. MW DDA and wind refers to the MarsWRF model Dust Devil Activity index and wind at 12–13 LMST (see text). Note that values pertain to annual statistics at a lander location, regardless whether the mission itself survived a full year. Wind speeds are m/s.

Mission	Pathfinder	Spirit	Opportunity	Phoenix	Curiosity	InSight
N. Latitude (°)	19.1	−14.6	−2.0	68.2	−4.6	4.5
E. Longitude (°)	−33.2	175.5	354.5	234.2	137.4	135.6
L_s Landing (°)	142.7	327.6	339	76.6	150.6	295.5
MCD Dust	7.3	6.8	7.6	5.1	6.0	7.0
MCD Ave Wind	10.1	7.3	4.3	11.5	5.6	10.5
MCD Max Wind	17.8	14.6	6.9	27	13.6	21.3
MCD Max PBL	5.2	5.7	5.7	4.55	5.3	4.5
MCD Ave Flux	0.31	0.32	0.31	0.08	0.33	0.37
MW Ave DDA	0.85	1.11	1.0	0.1	0.502	1.0
MW Max DDA	1.33	2.29	1.6	0.57	0.78	1.9
MW Ave Wind	5.0	4.1	2.7	5.5	5.0	
MW Max Wind	10.8	8.2	6.5	12.6	9.6	

those predicted for the general area, due to the effects of the significant regional-scale topography. In particular, maximum wind speeds are predicted to be very strong at night in southern summer (Rafkin et al., 2016; Vicente-Retortillo et al., 2018; Baker et al., 2018), a finding supported by Curiosity's observations of nighttime aeolian activity during primarily this portion of the year (Baker et al., 2018, 2021b, 2021b). Although Curiosity wind data suffer from many data gaps (e.g. Newman et al., 2017), Vicente-Retortillo et al. (2018) used high-resolution MarsWRF model output to show a correlation between dust cleaning periods and both strong predicted nighttime winds and high dust devil activity index. Hence strong winds, at night rather than during the daytime periods when convective vortices peak, may be responsible for direct cleaning events on some missions. Also, note that Phoenix mean and maximum wind speeds are larger than at InSight, averaged over a year, while Phoenix showed rapid removal initially; this points to a need to consider seasonal variations rather than annual averages for a more complete understanding in future studies.

It is of note, however, that the InSight 'lull' between Sols 200 and 400 is associated with a higher dust devil activity index predicted by the MarsWRF model (see Baker et al., 2021), and indeed the number of moderate (>0.5 Pa) and large (>2 Pa) pressure drops associated with convective vortices (Spiga et al., 2021) that were detected by InSight's instrumentation were roughly a factor of 2 higher than in the Sol 0–200 period. Thus, while InSight has observed neither large cleaning events nor camera-visible dust devils (Lorenz et al., 2021), the enhanced vortex activity in the Sol 200–400 period (L_s~45–110°) may have been enough to cause "micro-cleanings" that balanced the dust accumulation.

5.2. Comparison with other landed Mars measurements

It was remarked during the Viking mission, with the first lander views of a rock-strewn landscape, that for cm-scale rocks to remain unburied even after tens of thousands of years of dust accumulation, some process must also remove this dust (e.g. Guinness et al., 1982).

Lander/rover observations of dust accumulation on spacecraft surfaces relies on imaging with uniform illumination geometry (or at least, correction for illumination geometry, including the effects of different geometry and atmospheric dust optical depth). In some cases, suitable imaging is acquired only infrequently, but the observations do establish some consistency with the solar array observations reported here. The different interpretations of dust factor here, versus change in reflectance observed by cameras, in terms of the equivalent dust thickness is beyond the scope of the present paper.

The deposition of dust on exposed spacecraft surfaces (a few microns per year) was observed directly by the cameras on the Viking landers (e.g. Arvidson et al., 1983). Vaughan et al. (2010) report observations of other surfaces on the Mars Exploration Rovers, including the solar arrays and dust capture magnets. They noted that dust tended to form aggregates (up to mm size) on the lander deck and arrays, and that these aggregates would be more easily entrained by wind than the dust particles themselves.

In a 10-year study of the camera calibration targets on the Mars Exploration Rovers, Kinch et al. (2014) found an average dust deposition rate of 0.004±0.001, in units of optical depth. They noted that the dust deposition and removal cycle was different between Spirit and Opportunity: at Opportunity, dust removal tended to occur via gradual removal in two seasons, whereas for Spirit, removal occurred in brief, strong events which happened in one half of the year. Lorenz and Reiss (2015) showed that the Spirit events were consistent with the seasonal timing of dust devils.

Drube et al. (2010) observed settling rates on a sweep magnet deposition target on the Phoenix lander, and reported deposition rates expressed as 1.08 μm/Sol on the magnets, and 0.06 μm/Sol on magnetically-protected areas.

Yingst et al. (2020) reported observations of the dust cover on the Curiosity Mars Hand Lens Imager (MAHLI) calibration target. The MAHLI target was vertically-oriented, which was expected to reduce dust deposition compared with a horizontal surface on which airfall dust could be directly deposited. They found a mean dust coverage of 4.7% as a result of the balance of deposition and removal, estimating a removal rate of 2–4% per Sol. The evolution of the dust coverage was not uniform with time, and they explore the possibility that proximity to sand dunes might affect removal processes. A maximum dust coverage of 49% was observed during a major dust storm. Ordóñez-Etxeberria et al. (2020) found that the number of dust devils observed by Curiosity increased in the second and especially third Mars years of the mission: this may have enhanced removal, but could also have been associated with higher dust deposition. Interpretation of these Curiosity observations is not simple, and not straightforward to reconcile with the apparent jump in uncleaned dust factor evolution in Fig. 6c.

5.3. Comparison with Earth

In fact, terrestrial solar panels in arid regions show a similar pattern of behavior to that on Mars: slow accumulation of dust degrades output, but the dust is removed via episodic cleaning events. In this case, however, the cleaning events are usually rainfall, and usually the cleaning is near-total. Piliougine et al. (2013) show a time series of normalized short-circuit currents on cells under test in Southern Spain, and during the dry summer months, the output fell by up to 10% per month (i.e. 0.3% per day). A survey by Sarryah et al. (2014) shows that this is typical, with similar values reported in Libya, Nigeria and California, although a few places (Saudi Arabia, Kuwait, Bangladesh) have reported loss up to ~1.1% per day, presumably as a result of enhanced deposition associated with dust storms.

6. Conclusions

A simple 0.2% per Sol decay in solar array output for a given illumination is consistent with the long-term record on prior missions, assuming no dust removal. This expression is recommended as a best estimate, and is what was observed on InSight and is, remarkably, just what was predicted by Landis (1996) before any solar-powered landers: 'at the end of two years, in the baseline case, the remaining power is barely a quarter of the initial power'. A conservative approach to future solar powered missions should also allow for periods of several weeks where decay can be of the order of 1.0% per Sol.

The character of dust removal processes is quite different for the four missions for which a long-term record exists. Vigorous removal occurred on Spirit, with a strongly seasonally-repeating pattern. A somewhat similar pattern was observed on Curiosity. Frequent cleaning events also occurred for Opportunity, whereas almost none occurred on InSight (although a period of low net accumulation did occur). The inter-mission variation is consistent – perhaps counterintuitively - with background winds being stronger for InSight, and the boundary layer depth being shallower there. These indications show some promise that global and mesoscale models may be able to predict the frequency of cleaning events, but a full study of which meteorological parameter (or more likely, which combination of meteorological parameters) is the best predictor remains for future work. The collation of solar array observations in this paper serves as a benchmark for such an analysis. The annual mean and maximum Dust Devil Activity metric appear not to be effective predictors of the difference between InSight and the other missions (e.g. these DDA statistics are the same for InSight as for Spirit and Opportunity, yet the dust clearing events were prominent at the latter locations and absent for InSight).

This paper has considered dust as a uniform material. However, it is known that dust particle size can vary (being larger in association with nearby dust lifting) and the susceptibility to removal may similarly vary. Further, variations in humidity (e.g. the potential for deposition of frost at night on solar arrays) could influence the texture and adhesion of dust. Thus, neither prediction schemes nor mitigation measures may be universally successful. Conceivably the surface or atmospheric electrical conductivity could influence the effectiveness of electrostatic effects which may be important in dust adhesion. It is possible that local terrain variations could affect dust removal: possible effects could include the availability of more easily-saltated to abrade dust from panels (see also Yingst et al., 2020), surface roughness (which controls the boundary layer wind profile), or albedo or thermal inertia variations that might stimulate vortex formation.

A detailed consideration of dust mitigation schemes introducing additional hardware such as electrostatic or ultrasonic dust removal, gas jets etc. is beyond the scope of this paper. However, some simple geometric aspects of solar arrays that deserve consideration to maximize long-term performance include sloping the arrays, and having them close to the surface such that saltating sand grains may more easily reach their upper surface where they may abrade dust away.

Author statement

Ralph Lorenz: Conceptualization, Investigation, Writing – Original Draft. German M. Martínez, Aymeric Spiga, A. Vicente-Retortillo, Claire E. Newman, Naomi Murdoch, Francois Forget, Ehouarn Millour, Thomas Pierron, Investigation, Writing – Reviewing and Editing.

Declaration of competing interest

The authors declare that they have no known competing financial interests or personal relationships that could have appeared to influence the work reported in this paper.

Acknowledgements

We thank the InSight science and engineering teams for useful discussions. RL and CEN acknowledge the support of the NASA InSight Participating Scientist Program via Grants 80NSSC18K1626 and 80NSSC18K1630, respectively. AVR is supported by AEI Project No. MDM-2017-0737 Unidad de Excelencia "María de Maeztu"- Centro de Astrobiología (INTA-CSIC)". AS, FF, EM, TP acknowledge the support of CNES, ESA and of ANR (MAGIS, ANR-19-CE31-0008-08). This is InSight Contribution Number 193. We thank Matt Golombek and Veronique Ansan for useful comments.

Appendix 1. Expression and Portrayal of Dust Factor Evolution

Following previous work, we use the succinct "X%/Sol" terminology to describe the evolution of the dust factor. Although in practice the distinction is not significant, it should be understood that this is a % per Sol (Martian Solar Day, 1.0275 days) not a terrestrial day. Furthermore, although one can reasonably interpret the rate in a linear manner for short periods (i.e. 0.2% per Sol for 10 Sols leads to a decline from 1.0 to 0.98), this should not be done for extended periods. 400 Sols does not lead to a 0.2 factor, but rather I(400)/I(0) = exp(0.002*400) ~ 0.998^400 = 0.449. Clearly, an exponential decay forms a straight line in a semilogarithmic plot. We show in Fig. A1 the same data as in Fig. 3, but in log-linear form, which clearly shows many linear segments.

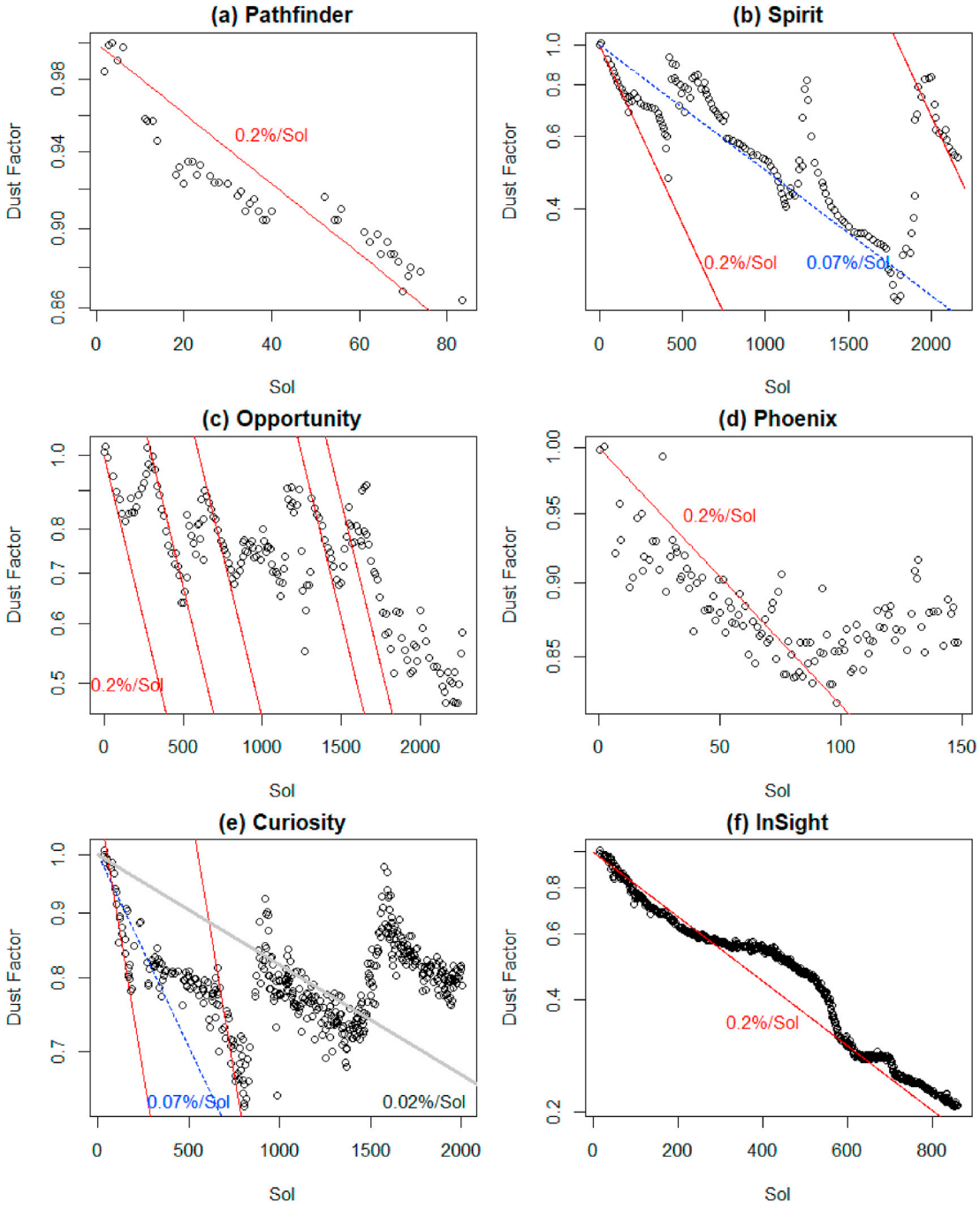

Fig. A1. Dust factor evolution as exponential decay (same data as Fig. 3, but with logarithmic y-axis). Exponential decays at 0.2%/Sol and a couple of representative values appear as straight lines. The net (accumulation minus removal) rates for Spirit and Curiosity can be ~3 or ~10x slower than 0.2%/Sol, but it is evident that this rate persists through most of the InSight record, and for many segments of Opportunity.

If the real decay rate of the array factor is d, and a characteristic noise on individual measurements is s, then the relative error in retrieved decay rate is ~s/nd, where n is the number of Sols between measurements. Thus, if s~1%, and d~0.2%, then estimates of d from sequential Sols (n = 1) will vary by a factor of several; the difficulties in interpreting this will be compounded if the measurement noise is non-Gaussian (as e.g. the quantization noise which affects the InSight measurement.) Thus, adopting a longer measurement interval (e.g. n = 5 as in section 4) brings more precise measurements. However, a longer measurement interval increases the probability that a cleaning event occurs in the measurement period, reducing the apparent measurement (or yielding a negative accumulation rate!). So some judgement is required for the InSight and Curiosity datasets. Since the other datasets were digitized by hand from published papers, the points were chosen to be sufficiently separated by eye that a difference estimate of the decay rate is reasonably accurate.

Appendix 2. Solar Array Shaking attempt on InSight

Given the accumulating dust on the InSight solar arrays, there was an attempt at around 12:14 LMST (10:20 UTC) on Feb 14, 2021 to remove the dust

on the solar arrays by activating the solar array deployment motors. The shaking lasted for approximately 20 s with the motor tugging on the arrays for 0.5 s at a time, followed by 0.5 s of pause. This led to effectively a 1 Hz vibration of the solar arrays.

Images of the solar arrays were taken before and after the shaking. During the shaking, 5 long exposure (500 ms) images were also taken, of which only one captured the array motion. The motion was observed to be a combination of rotational and side-to-side motion. By calculating the difference between two images of the solar arrays, we can estimate the amplitude of the motion to be ~10 pixels or ~2.2 cm at the array edge (Fig A2). As the image may not have captured the extremes of the array position, this may be a lower limit on the amplitude of motion induced by the shaking. We can, in turn, calculate the maximum shaking acceleration, a_s,following a_s = omega^2 * A, where omega is the frequency of vibration, and A is the amplitude of motion. This leads to a maximum (observed) acceleration of ~0.022 m/s^2 at 1 Hz, at the edge of the solar array.

From the before and after images, and also from the power generation data, there is no evidence of dust removal or dust motion. This implies that the adhesive force between the dust grains and the panels is larger than the force due to the shaking. Therefore, a 10 μm (1 μm) grain on the edge of the solar panel, with a grain density of 2 g/cm^3, must experience an adhesive force of at least 20 nN (0.2 nN) for no motion to be observed while shaking at ~0.022 m/s^2 with a frequency of 1 Hz. The low excitation frequency, coupled with the large adhesion to inertial force ratio for micron-sized particles, gives a low expectation for particle removal; however, the operations planning activity for this experiment were modest and it in any case also yielded desired information on array movements that were useful for seismic data interpretation.

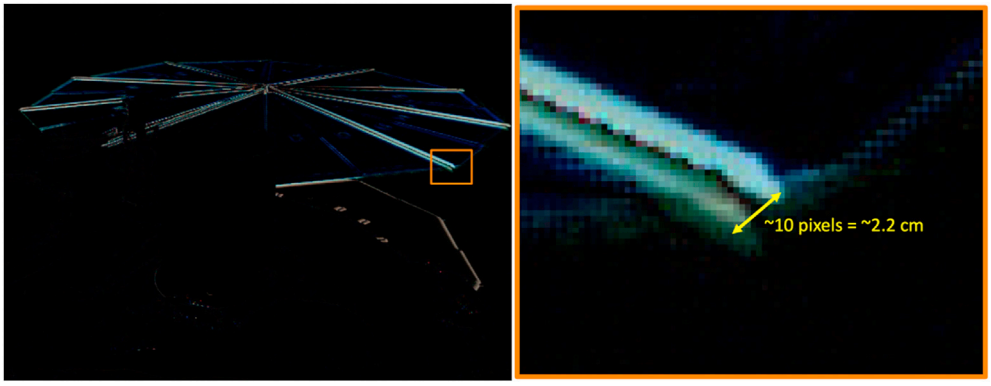

Fig. A2. (a) The difference between two images of the InSight solar arrays during shaking. (b) A close-up of the region indicated by the orange box in (a). The original images were taken by the InSight Instrument Deployment Camera (IDC) and are available here: https://mars.nasa.gov/insight/multimedia/raw-images/.

References

Arvidson, R.E., Guinness, E.A., Moore, H.J., Tillman, J., Wall, S.D., 1983. Three Mars years: viking lander 1 imaging observations. Science 222 (4623), 463–468.

Baker, M.M., Lapotre, M.G.A., Minitti, M.E., Newman, C.E., Sullivan, R., Weitz, C.M., et al., 2018. The Bagnold Dunes in southern summer: active sediment transport on Mars observed by the Curiosity rover. Geophys. Res. Lett. 45, 8853–8863. https://doi.org/10.1029/2018GL07904.

Baker, M., Newman, C., Charalambous, C., Golombek, M., Spiga, A., Banfield, D., Lemmon, M., Banks, M., Lorenz, R., Garvin, J., Grant, J., 2021. Vortex-dominated aeolian activity at InSight's landing site, Part 2: local meteorology, transport dynamics, and model analysis. J. Geophys. Res.: Plan. https://doi.org/10.1029/2020JE006514.

Charalambous, C., Ansan, V., Baker, M., Banerdt, W.B., Banfield, D., Banks, M., Daubar, I., Golombek, M., Grant, J., Hauber, E., Johnson, C., Lemmon, M., Lognonné, P., Lorenz, R., Lucas, A., Maki, J., McClean, J.B., Mittelholz, A., Moreiras, D.V., Murdoch, N., Navarro, S., Newman, C., Perrin, C., Pike, W.T., Pla-García, J., Rodriguez, S., Sotomayor, L., Spiga, A., Stott, A., Warren, T., Warner, N.H., Weitz, C., 2021. Vortex-dominated aeolian activity at InSight's landing site, Part 1: Multi-instrument Observations, Analysis and Implications. J. Geophys. Res. Plan. https://doi.org/10.1029/2020JE006757.

Coyne, J., Jackson, W., Lewicki, C., 2009. August. Phoenix electrical power subsystem-power at the martian Pole. AIAA-2009-4518. In: In 7th International Energy Conversion Engineering Conference, 2 - 5 August 2009, Denver, Colorado.

Crisp, D., Pathare, A., Ewell, R.C., 2004. The performance of gallium arsenide/germanium solar cells at the Martian surface. Acta Astronaut. 54 (2), 83–101.

Drube, L., Leer, K., Goetz, W., Gunnlaugsson, H.P., Haspang, M.P., Lauritsen, N., Madsen, M.B., Sørensen, L.K.D., Ellehoj, M.D., Lemmon, M.T., Morris, R.V., 2010. Magnetic and optical properties of airborne dust and settling rates of dust at the Phoenix landing site. J. Geophys. Res.: Plan 115 (E5). https://doi.org/10.1029/2009JE003419.

Ellehoj, M.D., Gunnlaugsson, H.P., Taylor, P.A., Kahanpää, H., Bean, K.M., Cantor, B.A., Gheynani, B.T., Drube, L., Fisher, D., Harri, A.M., Holstein-Rathlou, C., 2010. Convective vortices and dust devils at the Phoenix Mars mission landing site. J. Geophys. Res.: Planets 115 (E4). https://doi.org/10.1029/2009JE003413.

Fenton, L.K., Lorenz, R., 2015. Dust devil height and spacing with relation to the martian planetary boundary layer thickness. Icarus 260, 246–262.

Forget, F., Hourdin, F., Fournier, R., Hourdin, C., Talagrand, O., Collins, M., Lewis, S.R., Read, P.L., Huot, J.P., 1999. Improved general circulation models of the Martian atmosphere from the surface to above 80 km. J. Geophys. Res.: Plan 104 (E10), 24155–24175.

Gaier, J.R., Perez-Davis, M.E., Moinuddin, A.M., 1991. Effects of windblown dust on photovoltaic surface s on Mars. In: Proceedings of the 26th Intersociety Energy Conversion Engineering Conference, IECEC-91. American Nuclear Society, La Grange Park, Il, pp. 313–318. August 4-9, 199 Boston, MA.

Guinness, E.A., Leff, C.E., Arvidson, R.E., 1982. Two Mars years of surface changes seen at the Viking landing sites. J. Geophys. Res.: Solid Earth 87 (B12), 10051–10058.

Kahre, M.A., Murphy, J.R., Newman, C.E., Wilson, R.J., Cantor, B.A., Lemmon, M.T., Wolff, M.J., 2017. The Mars dust cycle. In: The Atmosphere and Climate of Mars. Cambridge University Press.

Kinch, K.M., Bell III, J.F., Goetz, W., Johnson, J.R., Joseph, J., Madsen, M.B., Sohl-Dickstein, J., 2015. Dust deposition on the decks of the Mars Exploration Rovers: 10 years of dust dynamics on the Panoramic Camera calibration targets. Earth Space Sci. 2 (5), 144–172.

Lam, G.Q., Billets, S., Norick, T., Warwick, R., 2016. Solar array design for the Mars InSight lander mission. In: 14th International Energy Conversion Engineering Conference July 25-27, 2016. Salt Lake City, UT. https://arc.aiaa.org/doi/pdf/10.2514/6.2016-4520.

Landis, G.A., 1996. Dust obscuration of Mars solar arrays. Acta Astronaut. 38 (11), 885–891.

Landis, G.A., Jenkins, P.P., 2000. Measurement of the settling rate of atmospheric dust on Mars by the MAE instrument on Mars Pathfinder. J. Geophys. Res.: Plan 105 (E1), 1855–1857.

Lemmon, M.T., Wolff, M.J., Bell III, J.F., Smith, M.D., Cantor, B.A., Smith, P.H., 2015. Dust aerosol, clouds, and the atmospheric optical depth record over 5 Mars years of the Mars Exploration Rover mission. Icarus 251, 96–111.

Lisano, M.E., Kallemeyn, P.H., 2017. March. Energy management operations for the Insight solar-powered mission at Mars. In: *2017 IEEE Aerospace Conference* Big Sky, MT March 2017. https://doi.org/10.1109/AERO.2017.7943965.

Lorenz, R.D., Reiss, D., 2015. Solar panel clearing events, dust devil tracks, and in-situ vortex detections on Mars. Icarus 248, 162–164.

Lorenz, R.D., Jackson, B.K., 2016. Dust devil populations and statistics. Space Sci. Rev. 203, 277–297. https://doi.org/10.1007/s11214-016-0277-9.

Lorenz, R.D., Lemmon, M.T., Maki, J., Banfield, D., Spiga, A., Charalambous, C., Barrett, E., Herman, J.A., White, B.T., Pasco, S., Banerdt, W.B., 2020. Scientific observations with the InSight solar arrays : dust, clouds and eclipses on Mars. Earth Space Sci. https://doi.org/10.1029/2019EA000992.

Lorenz, R.D., Spiga, A., Lognonné, P., Plasman, M., Newman, C.E., Charalambous, C., 2021. The whirlwinds of Elysium: a catalog and meteorological characteristics of "dust devil" vortices observed by InSight on Mars. Icarus, 114119.

Madeleine, J.B., Forget, F., Millour, E., Montabone, L., Wolff, M.J., 2011. Revisiting the radiative impact of dust on Mars using the LMD global climate model. J. Geophys. Res.: Plan 116 (E11). https://doi.org/10.1029/2011JE003855.

Martínez, G.M., Newman, C.N., De Vicente-Retortillo, A., Fischer, E., Renno, N.O., Richardson, M.I., Fairén, A.G., Genzer, M., Guzewich, S.D., Haberle, R.M.,

Harri, A.M., 2017. The modern near-surface Martian climate: a review of in-situ meteorological data from Viking to Curiosity. Space Sci. Rev. 212 (1), 295–338.
Newman, C.E., Kahanpää, H., Richardson, M.I., Martínez, G.M., Vicente-Retortillo, A., Lemmon, M.T., 2019. MarsWRF convective vortex and dust devil predictions for Gale Crater over 3 Mars years and comparison with MSL-REMS observations. J. Geophys. Res.: Plan 124 (12), 3442–3468.
Murphy, J.R., Nelli, S., 2002. Mars Pathfinder convective vortices: Frequency of occurrence. Geophys. Res. Lett. 29 (23), 18–1.
Newman, C.E., De La Torre Juarez, M., Pla-García, J., Wilson, R.J., Lewis, S.R., Neary, L., Kahre, M.A., Forget, F., Spiga, A., Richardson, M.I., Daerden, F., 2021. Multi-model meteorological and aeolian predictions for Mars 2020 and the jezero crater region. Space Sci. Rev. 217 (1), 1–68. https://doi.org/10.1007/s11214-020-00788-2.
Ordóñez-Etxeberria, I., Hueso, R., Sánchez-Lavega, A., 2020. Strong increase in dust devil activity at Gale crater on the third year of the MSL mission and suppression during the 2018 Global Dust Storm. Icarus 347, 113814.
Perrin, C., Rodriguez, S., Jacob, A., Lucas, A., Spiga, A., Kawamura, T., Murdoch, N., Pan, L., Lorenz, R., Daubar, I.J., Lognonne, P., Banfield, D., Banks, M.E., Garcia, R.F., Newman, C., Ohja, L., Widmer-Schnidrig, R., Banerdt, W.B., 2020. Monitoring of dust devil tracks around the InSight landing site, Mars, and comparison with in-situ atmospheric data. Geophys. Res. Lett. 47. https://doi.org/10.1029/2020GL087234.
Piliougine, M., Cañete, C., Moreno, R., Carretero, J., Hirose, J., Ogawa, S., Sidrach-de-Cardona, M., 2013. Comparative analysis of energy produced by photovoltaic modules with anti-soiling coated surface in arid climates. Appl. Energy 112, 626–634.
Rafkin, S.C., Pla-Garcia, J., Kahre, M., Gomez-Elvira, J., Hamilton, V.E., Marín, M., Navarro, S., Torres, J., Vasavada, A., 2016. The meteorology of Gale crater as determined from rover environmental monitoring station observations and numerical modeling. Part II: interpretation. Icarus 280, 114–138.
Reiss, D., Lorenz, R., 2016. Dust devil track survey at elysium planitia, Mars : implications for the InSight landing sites. Icarus 266, 315–330.
Rennó, N.O., Burkett, M.L., Larkin, M.P., 1998. A simple thermodynamical theory for dust devils. J. Atmos. Sci. 55 (21), 3244–3252.
Sayyah, A., Horenstein, M.N., Mazumder, M.K., 2014. Energy yield loss caused by dust deposition on photovoltaic panels. Sol. Energy 107, 576–604.
Spiga, A., Murdoch, N., Lorenz, R., Forget, F., Newman, C., Rodriguez, S., Pla-Garcia, J., Viúdez-Moreiras, D., Banfield, D., Perrin, C., Mueller, N.T., 2020. A Study of Daytime Convective Vortices and Turbulence in the Martian Planetary Boundary Layer Based on Half-A-Year of InSight Atmospheric Measurements and Large-Eddy Simulations arXiv preprint arXiv:2005.01134.
Stella, P.M., Herman, J.A., 2010. June. The Mars surface environment and solar array performance. In: 2010 35th IEEE Photovoltaic Specialists Conference. IEEE, 002631-002635.
Stella, P.M., Chin, K., Wood, E., Herman, J., Ewell, R., 2009. June. Managing PV power on Mars—MER rovers. In: 2009 34th IEEE Photovoltaic Specialists Conference (PVSC). IEEE. https://doi.org/10.1109/PVSC.2009.5411206, pp. 001073-001078.
Team, R., 1997. Characterization of the martian surface deposits by the Mars pathfinder rover. Sojourner. Sci. 278 (5344), 1765–1768.
Vaughan, A.F., Johnson, J.R., Herkenhoff, K.E., Sullivan, R., Landis, G.A., Goetz, W., Madsen, M.B., 2010. Pancam and Microscopic Imager Observations of Dust on the Spirit Rover: Cleaning Events, Spectral Properties, and Aggregates *Mars*, vol. 5, pp. 129–145. https://doi.org/10.1555/mars.2010.0005.
Vicente-Retortillo, Á., Martínez, G.M., Renno, N., Newman, C.E., Ordonez-Etxeberria, I., Lemmon, M.T., et al., 2018. Seasonal deposition and lifting of dust on Mars as observed by the Curiosity rover. Sci. Rep. 8 (1), 1–8. https://doi.org/10.1038/s41598-018-35946-8.
Viúdez-Moreiras, D., Newman, C.E., Forget, F., Lemmon, M., Banfield, D., Spiga, A., Lepinette, A., Rodriguez-Manfredi, J.A., Gómez-Elvira, J., Pla-García, J., Muller, N., 2020. Effects of a large dust storm in the near-surface atmosphere as measured by InSight in elysium planitia, Mars. Comparison with contemporaneous measurements by Mars science laboratory. J. Geophys. Res.: Plan 125 (9) e2020JE006493.
Yingst, R.A., Bray, S., Herkenhoff, K., Lemmon, M., Minitti, M.E., Schmidt, M.E., et al., 2020. Dust cover on Curiosity's Mars Hand Lens Imager (MAHLI) calibration target: implications for deposition and removal mechanisms. Icarus, 113872.